

Evaluation of the Imprio 100 Step and Flash Imprint Lithography Tool

Kathleen A. Gehoski, David P. Mancini, Douglas J. Resnick
Microelectronics and Physical Sciences Laboratories, Motorola Labs, Tempe, AZ USA 85284

ABSTRACT

Step and Flash Imprint Lithography (S-FIL) is one of several new methods of imprint lithography being actively developed. As with other nanoimprint methods, S-FIL resolution appears to be limited only by template resolution, and offers a significant cost of ownership reduction when compared to other NGL methods such as EUVL and 157 nm lithography. Market segments capable of being addressed with S-FIL technology include nanodevice fabrication, compound semiconductors, photonic and optical devices, data storage, and advanced packaging. Successful implementation will require a commercial supplier of S-FIL tools, as well as an infrastructure that will support fabrication of the necessary 1X templates. The Imprio 100, manufactured by Molecular Imprints, Inc. is the first commercially available S-FIL tool. The purpose of this paper is to describe the performance and capabilities of the Imprio 100.

Performance related to several tool parameters including layer-to-layer overlay, pre-aligner precision, residual layer thickness and uniformity, resolution, wafer throughput, and exposure lamp intensity uniformity was evaluated. Several spin-coatable organic materials were evaluated for their efficacy as transfer layers. Contact angle analysis of each material along with a comparison of the spread time and resulting residual layer, and overall resolution using each material was also done. This paper will present the results of both the factory and site acceptance tests, and will also cover the imprinting capability of the tool.

KEY WORDS: Step and Flash Imprint Lithography, S-FIL, Imprio 100, template

1. INTRODUCTION

With the 2003 inclusion of nanoimprint lithography to the International Technology Roadmap for Semiconductors (ITRS), imprint technology has received industry acceptance as a viable Next Generation Lithography (NGL), with the potential to be inserted into manufacturing at the 32 nm node by 2013.¹

There are two broad category methods of nanoimprint lithography that use rigid templates to achieve ultra-high resolution features. The first is thermal imprinting where the material to be imprinted is polymeric, and is first taken above its glass transition temperature (T_g) to soften it making it malleable to a template relief surface.² The template is pressed into the softened film under pressures that can exceed 10 atmospheres. The mold and substrate are then cooled to below the T_g to release the template and create the pattern.

The second method involves the use of UV-curable monomeric materials. There are two methods of depositing the UV curable material. These include a spin-on type applied prior to imprinting as with a conventional resist, and a point-of-use type, dispensed just prior to imprinting a field.³ With the spin-on process, the material must remain wet. Forming a stable, wet layer requires low molecular weight polymers that inevitably have a high viscosity, which consequently necessitate very high pressures during imprinting. The field-to-field method, employed in S-FIL, is achieved by dispensing a UV-curable monomer immediately before a transparent template is pressed into contact with that particular field.⁴ Since the material is of low viscosity it does not require high pressures to cause it to flow into the relief surface of a template. The material is then cured with a broadband light source before the template and wafer are separated. The term Step and Flash Imprint Lithography (S-FIL) is derived from the stage positioning step and dispense of the monomer and the flash of the Hg ARC lamp.

With its ability to operate at both room temperatures and ambient pressures, and its transparent templates, S-FIL offers the advantages of improved overlay and resolution performance independent of

pattern density. S-FIL is a replication technique that has the potential to lead to low cost and high throughput. It has been shown that the resolution of the process is only limited to the resolution of the template, and can be as good as 20 nm.⁵

Molecular Imprints Inc. first commercially available S-FIL tool, the Imprio 100, was delivered to Motorola in July 2003 (Figure 1). The step-and-repeat operation for first layers is automated, and alignment of second layers is done by an operator on a die-by-die basis.⁶ The through-the-template single die alignment system, performed in proximity mode, allows for registration of better than 500 nm. This paper will present the results of both the factory and site acceptance tests, and will also cover the imprinting capability of the tool.



Figure 1. Imprio 100 S-FIL system from Molecular Imprints Inc.

1.1 Imprio 100 tool features

The Imprio 100 has a single wafer, semi-automated wafer handler that is capable of loading and unloading wafer sizes of 100 mm, 150 mm, and 200 mm. A semi-automated template handler is available for loading and unloading the 65 mm × 65 mm × 0.25" templates. The Imprio 100 is equipped with a dual dispense system for two different monomers, along with supporting hardware and software to permit the user to select monomer drop pattern recipes. The monomer is cured using an Hg ARC lamp source manufactured by Optical Associates Inc. The Graphical User Interface (GUI) is very user-friendly for operating the system to create engineering programs. The die-by-die alignment feature allows the operator to align, through the template, each individual die with alignment accuracy largely dependant upon the skill of the operator. A single template chuck holds the template, which is used to print fields having a maximum dimension of 25 mm × 25 mm. The Imprio 100 has a self-contained, class 0.1 mini-environment to minimize the introduction of particles.

2. EXPERIMENTAL

Templates were fabricated on standard 6" × 6" × 0.25" (6025) quartz mask blanks supplied by Ulcoat USA, Inc. Chromium films were deposited onto mask blanks using an MRC 603A sputtering system. A Leica VB6 electron beam exposure system with a thermal field emitter source operating at a beam accelerating voltage of 100 keV was used for all exposures. Coating and baking of templates was done on EV Group model 150/160 coat and bake tracks, and ZEP 520A positive e-beam resist supplied by Zeon

Chemical was used throughout. All dry etches including etches of resist scum, chromium films, and quartz template relief were done in a Unaxis VLR tool.⁷ Templates were cut from the 6025 quartz plate by American Precision Dicing using a diamond saw. Cross-sectional SEM photos were taken using a Hitachi S4500 SEM. Overlay and registration accuracy was measured on the Leica LMS2020. Residual layer thickness measurements were gathered using the Nanometrics model 210XP. Contact angles were measured with a laboratory-manufactured goniometer with ImageJ software obtained by NIH. First level patterned wafers were exposed on a ASML Micrascan III. All work was done on 200 mm silicon wafers coated with either of the following materials: Brewer Sciences DUV30J, Shipley AR2450, and MicroChem SF6 (poly)methyl glutarimide (PMGI). Coating and baking of wafers was done on a Karl Suss ACS200 or SVG90S.

Templates were cleaned and treated using the following materials: isopropyl alcohol, sulfuric acid, and hydrogen peroxide. A Branson 8000 oxygen ashers is also used to remove organic materials from template surfaces. Templates were coated with RelMat™, a release agent supplied by Molecular Imprints Inc.

3. RESULTS AND DISCUSSION

3.1 Registration and overlay

Two alignment measurement tests were performed: registration of a first pattern layer, and overlay of a second pattern layer aligned to first pattern, which was etched into the substrate. A template is first loaded into its chuck and leveled using the automated leveling system. Template rotation is removed by first printing a single die into a test wafer, and using a built-in microscope to sight alignment marks located on the extreme left and right sides of the field. Die are printed and the template theta adjusted iteratively until these marks are in alignment with the X-travel of the stage. In the registration test, fields are imprinted blindly across an entire wafer with a known stepping distance between each field. Their locations are measured and plotted to provide a fingerprint of the precision of stage positioning.

A grid registration wafer was imprinted and then analyzed on an LMS2020 to determine the stage fingerprint. Figure 2 represents the findings. The magnification error has been removed from this data.

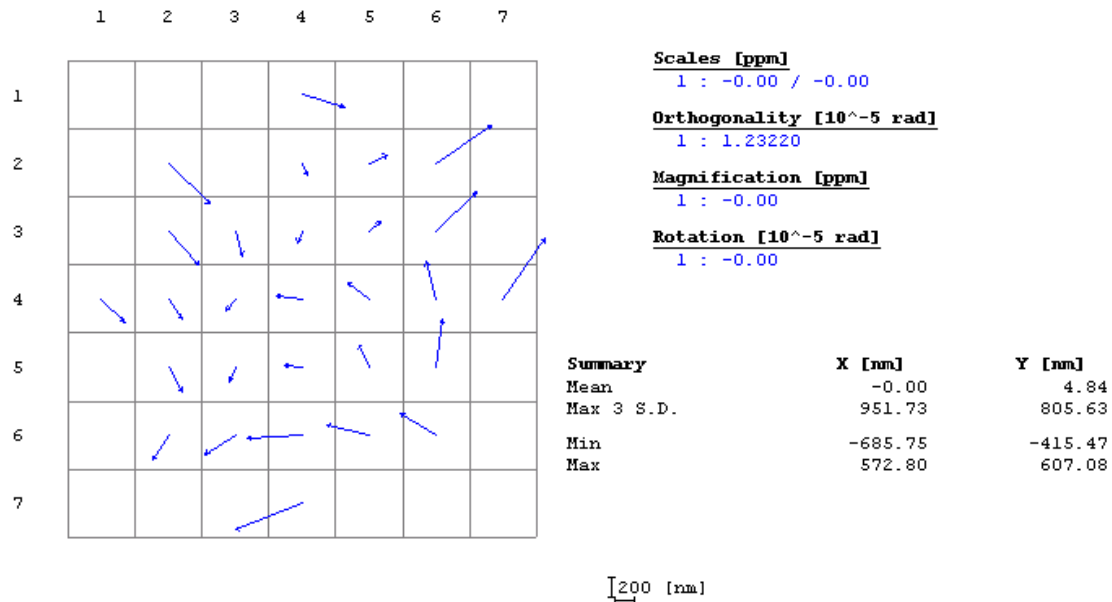


Figure 2. LMS2020 Registration analysis

Alignment is performed on a die-by-die basis under the complete control of an operator. Figure 3 depicts the alignment pattern that was used. A Moire pattern is included and can be used to make final alignment corrections. The LMS2020 uses the box-in-box alignment patterns to determine the overlay error from the inner box (1st pattern) to the outer box (2nd pattern).

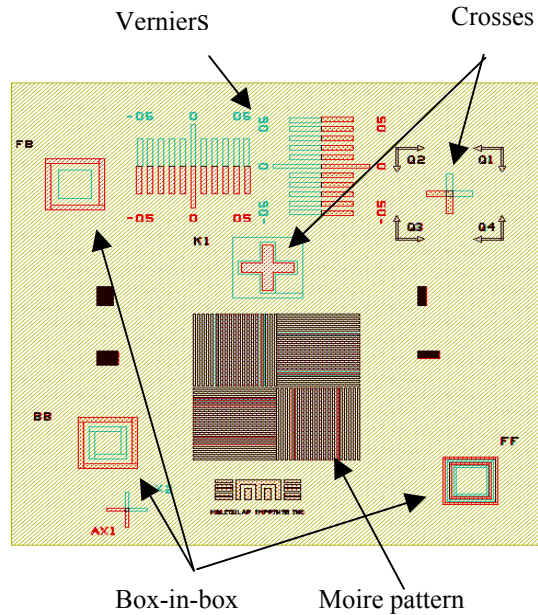


Figure 3. Alignment pattern

The first alignment test performed involved using the Imprio 100 to align to wafers that had been first-pattern imprinted by the Imprio 100 itself. Table 1 shows the data gathered from this test. The data is taken from readings of vernier patterns located in three places on each imprinted field. The Imprio 100 specification for overlay is 500 nm 3σ . All three wafers were within this specification.

Wafer	X (NM)	Y (NM)	3 sigma X	3 sigma Y
1	-94	46	371	347
2	-19	-16	282	265
3	-17	35	228	217

Table 1. Vernier overlay data for three wafers from Imprio 100 to itself.

The second alignment test involved wafers which had been first-patterned on an ASML Micrascan III (MS III) DUV scanner. As with the first test, die-by-die alignment was performed for each field and the second pattern imprinted using the Imprio 100. Figures 4 and 5 show the LMS2020 analysis of overlay error of the Imprio 100 to the MS III for two different wafers. The Imprio 100 was able to achieve less than 500 nm in both X and Y 3σ . In one case, alignment results in x and y were well below 200 nm, 3σ .

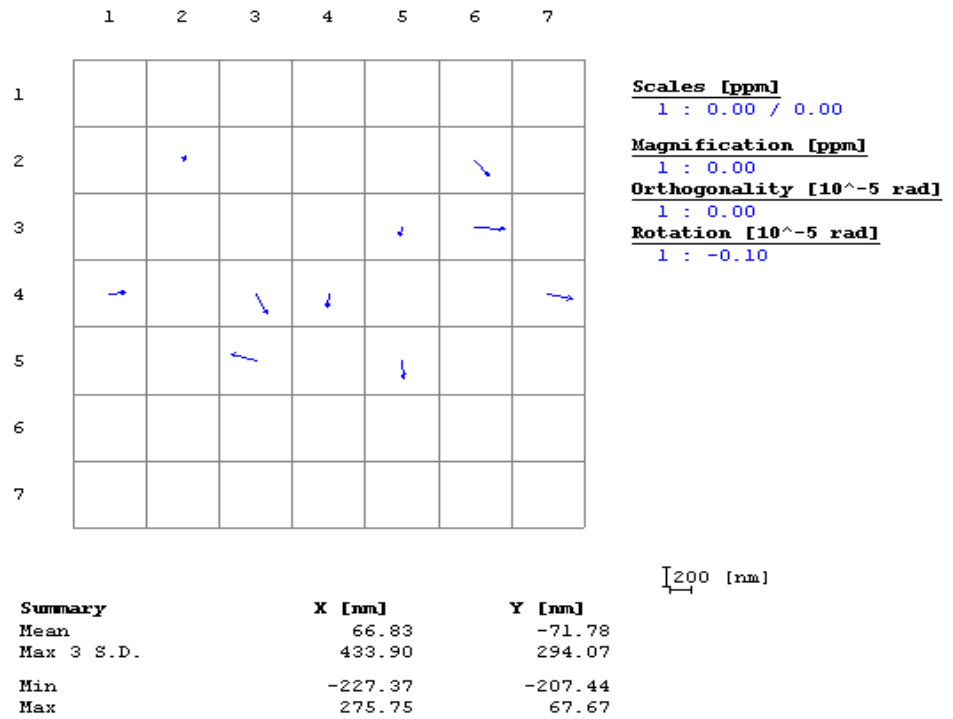


Figure 4. Wafer #1 LMS2020 data: MS III to Imprio 100 overlay

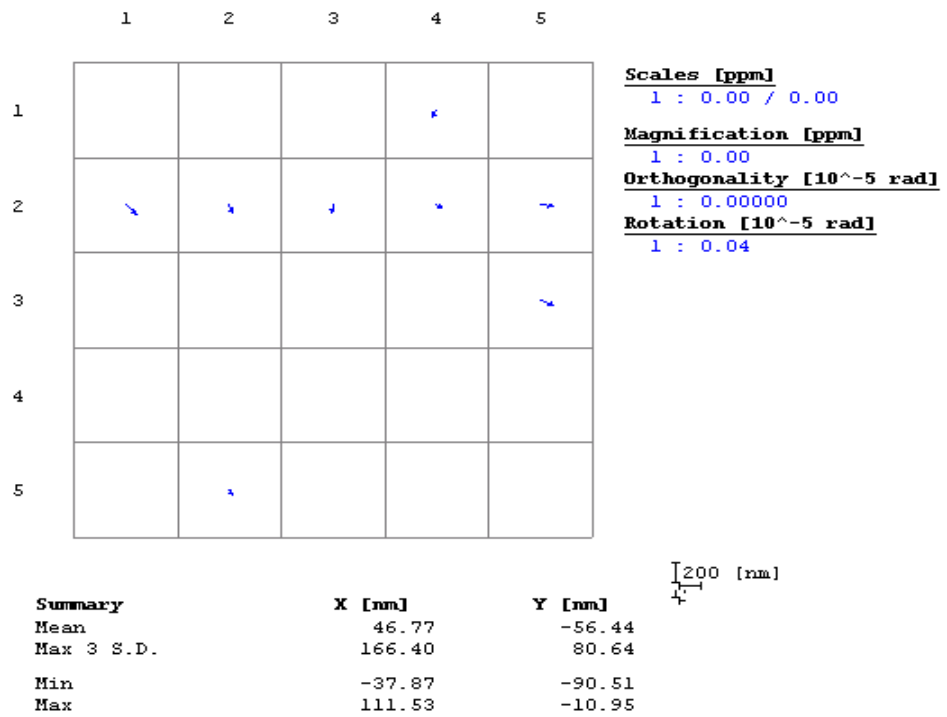


Figure 5. Wafer #2 LMS2020 data: MS III to Imprio 100 overlay

Although each 200 mm wafer had 29 die imprinted, the LMS2020 had difficulty distinguishing the box-in-box alignment mark of the etch barrier with that of the etched silicon. This is the reason several die are missing from the plot.

3.2 Residual Layer

Just prior to curing, etch barrier monomer is being pressed into contact with the transfer layer where it flows across the surface of the template and fills its relief contours. Due to viscous forces, a residual of etch barrier monomer remains since it is not possible to expel all unnecessary material from the active (print) region of the template. When irradiated, this residual layer cures and remains as a film between the printed features and the transfer layer. Maintaining the uniformity of the residual layer is critical since pattern transfer of features to the substrate must include a timed etch of the residual layer prior to etching the transfer layer. Residual layers that are non-uniform or that vary from die-to-die will not be etched completely (if too thick) or will be over-etched (if too thin). The residual layer uniformity specification for the Imprio 100 is 50 to 150 nm 3σ . The system was able to achieve 70 to 100 nm 3σ with a constant spread time of 130 seconds on a Brewer Science DUV30J transfer layer. Figure 6 shows the results of this test.

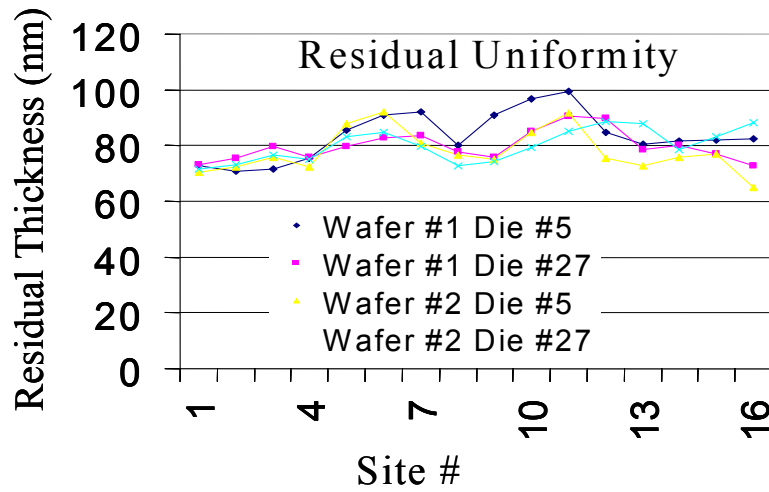


Figure 6. Residual layer uniformity on Brewer Science DUV30J

Two additional materials were explored as transfer layers: Shipley AR2450 and MicroChem SF6 PMGI. Shipley AR2450 is a material designed to have good etch resistance as the underlayer of a bi-layer resist scheme. MicroChem SF6 is routinely used as the underlayer of a bi-layer lift-off resist stack. As a result, either of these two materials can potentially be a good choice for the transfer layer depending upon the desired application. All three of the materials were tested for compatibility with the etch barrier.

Since the surface energy of the transfer layer can play a key role in the time required for etch barrier spreading, a water droplet contact angle test was done for each of the three candidate transfer layers. As a comparison of surface energies, a water droplet contact angle test was also done on a layer of cured etch barrier. In addition, the contact angle of a droplet of etch barrier monomer (uncured) was also measured on each transfer layer material. The resultant water droplet contact angles for the four materials tested are shown in Figure 7. The contact angle for the uncured etch barrier monomer was found to be less than 5° on all materials.

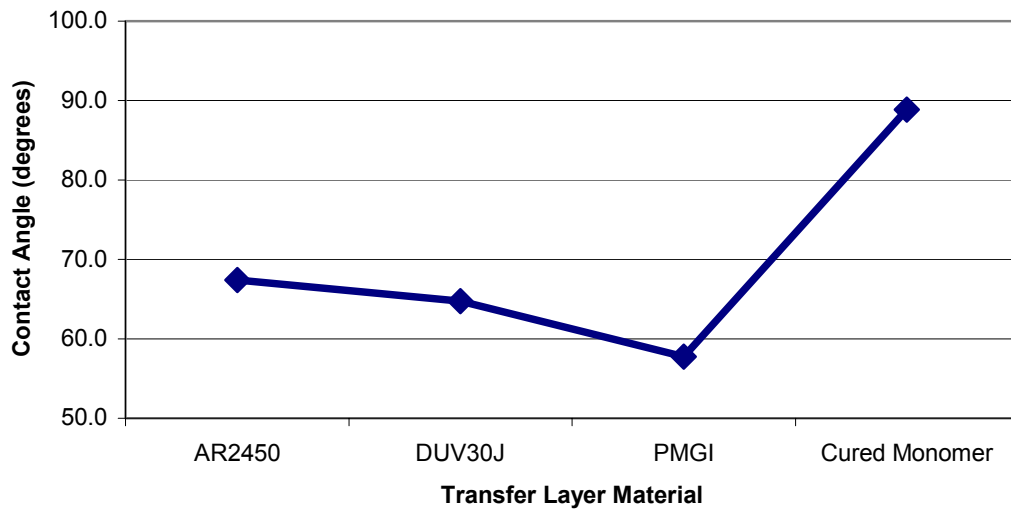


Figure 7. Contact angles of transfer layer materials with water droplets

An additional test was done on the three candidate transfer layer materials to determine how the resultant etch barrier layer thickness varied as a function of spread time. For each transfer layer material the spread time was varied from 5 seconds to 600 seconds. Residual layer thickness readings were taken across a single imprinted field in 15 places for each spread time. The results of these findings are seen in figures 8, 9, and 10.

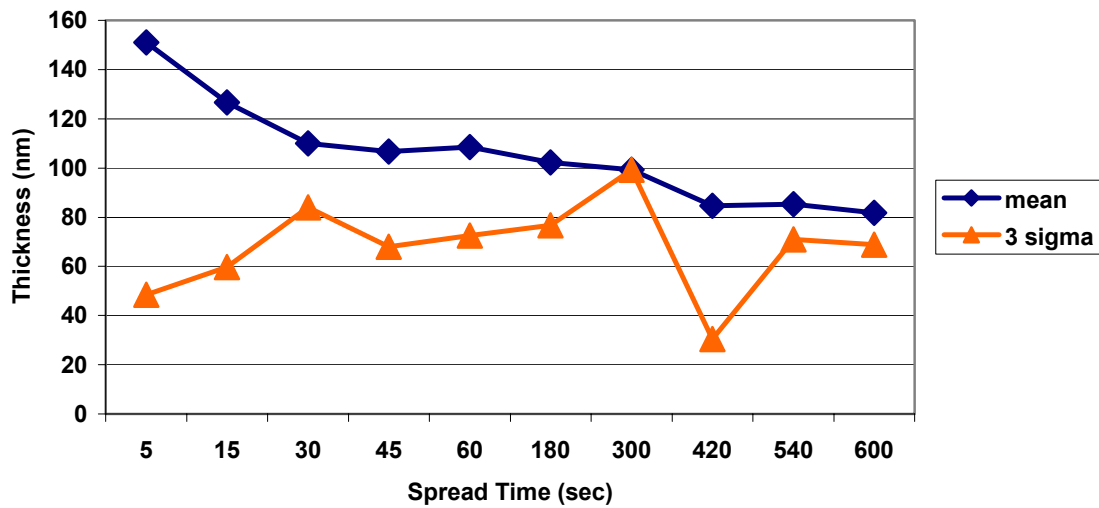


Figure 8. Residual layer uniformity on Brewer Science DUV30J

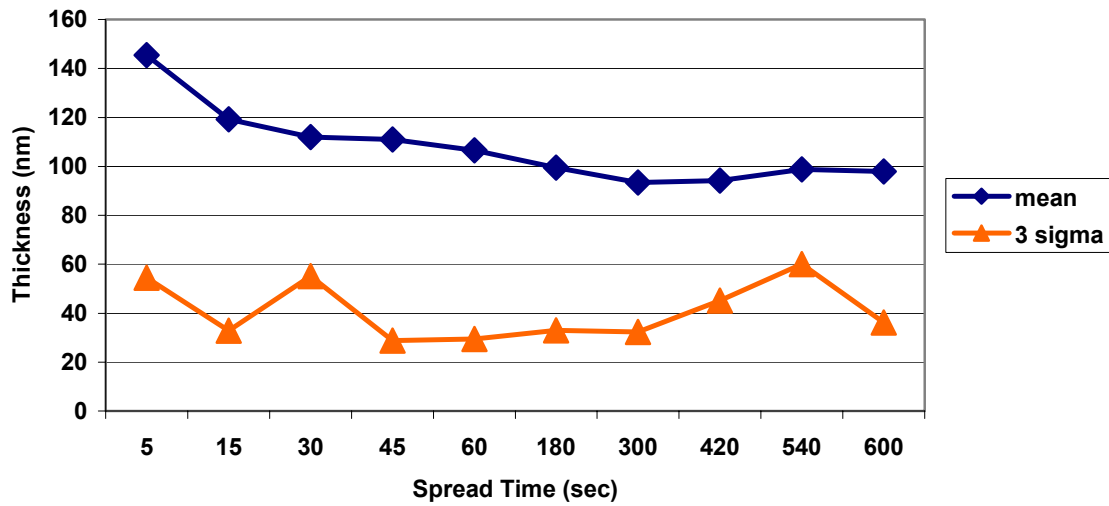


Figure 9. Residual layer uniformity on Shipley AR2450

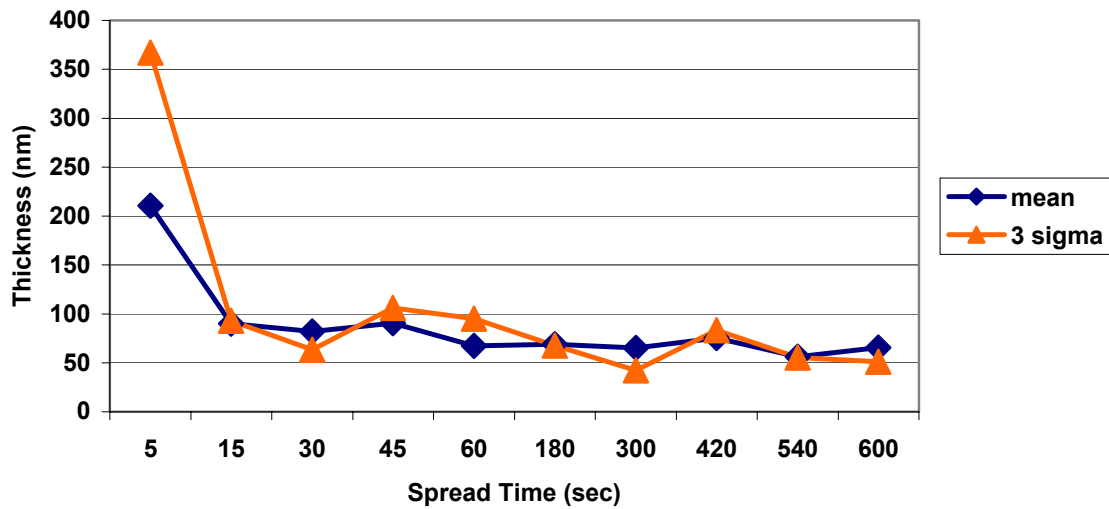


Figure 10. Residual layer uniformity on MicroChem SF6 (PMGI)

The test indicates that the residual layer thickness falls rapidly to a constant level below 120 nm in the first 30 seconds, but levels off after that, taking 100-300 additional seconds to fall consistently below 100 nm. The spread in the data reflected by 3σ values is high, but believed to be abnormally so due to incomplete spreading of etch barrier monomer for the shorter spread times.

From the results of the contact angle test and the spread time residual layer uniformity test, it appears that the etch barrier spreads faster and is more uniform for higher transfer layer surface energies, or the lower contact angles.

3.3 Print resolution and quality

The etch barrier material itself must be formulated to have a minimal viscosity to promote a rapid spreading. However, once cured it must release readily from the template without shearing cohesively or

debonding adhesively from the transfer layer. Some of these desired characteristics require material mechanical and physical properties, which are in conflict with each other. Finally, to promote dry etch selectivity relative to purely organic transfer layers, a maximum amount of silicon should be incorporated into the final formulation. As a result of all of these factors, chemists must accept performance compromises in these properties to achieve an acceptable formulation.

Figure 11 shows typical examples of resolved lines of 100 nm 1:1 pitch and 40 nm 1:1.5 pitch. Cross-sectional SEM micrographs of both feature sets show vertical sidewalls having $>85^\circ$ wall angles in agreement with measured template profiles. Feature height of approximately 80 nm is roughly 15 nm less than has been measured in the template. These results easily exceed the specification for resolution of the Imprio 100 of ≤ 100 nm with a 1:1 pitch. Also shown in Figure 11 is the boundary between transfer and etch barrier layer and a residual layer thickness of approximately 70 nm.

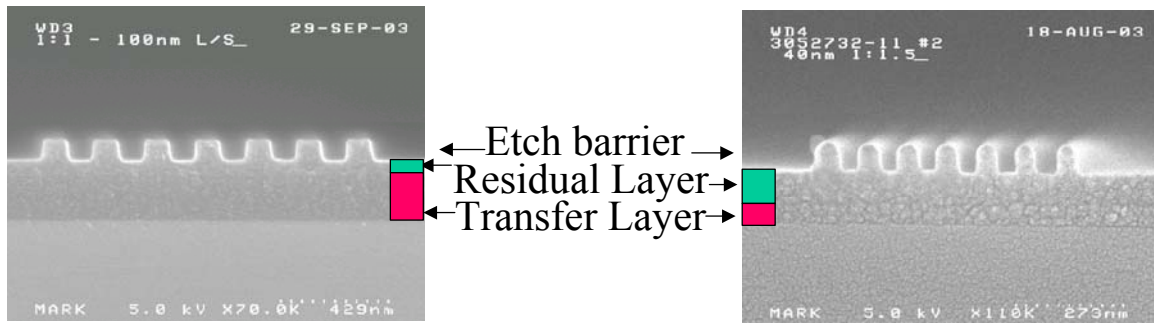


Figure 11a. 100 nm 1:1

Figure 11b. 40 nm 1:1.5

Figure 12 show cross-sectional SEM micrographs of each of the three transfer layer materials evaluated, printed with 70 nm features. Each cross-section shows good adhesion between etch barrier and transfer layers, with no image shearing or cohesive failure apparent.

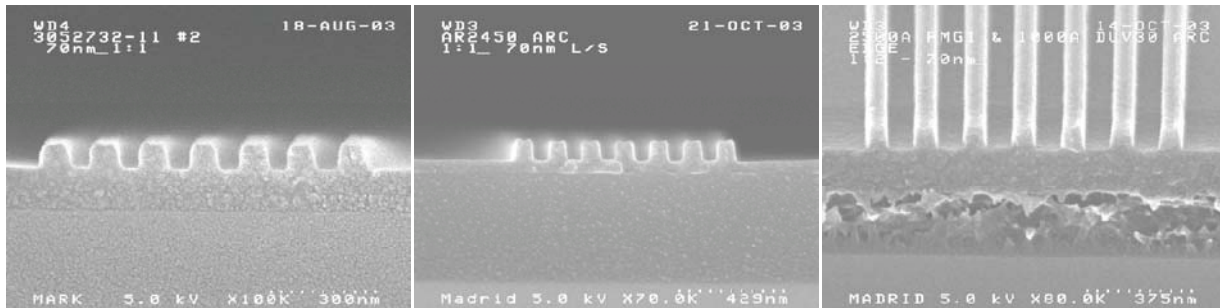


Figure 12a. Brewer Science DUV30J

12b. Shipley AR2450

12c. Micro Chem PMGI SF6

3.4 Miscellaneous specifications

The specification for lamp intensity non-uniformity was $< 15\%$ over the entire 25 mm field. During acceptance testing, the Imprio 100 was able to achieve a specification of $< 12.7\%$ non-uniformity. The automatic wafer handler pre-align precision specification was $\pm 200 \mu\text{m}$, mean $+ 3\sigma$. During acceptance testing, the Imprio 100 was able to achieve $53 \mu\text{m}$ in X and $108 \mu\text{m}$ in Y $+ 3\sigma$. The time required to change templates was specified to be < 30 minutes. This time requirement was easily met, but is operator dependent. The wafer throughput specification of two, 200 mm wafers having 37 imprinted fields per hour was not met. This was largely due to the excessive dispense and spread times used. In particular, spread times of typically 90-120 seconds were required to achieve the desire minimal residual layers of < 100 nm.

As a result, only a single 200 mm wafer per hour on average was achieved. Table 2 provides a summary of the specifications of the Imprio 100 and the corresponding results of acceptance testing.

Operation	MII Specification	Achieved
Hg Lamp non-uniformity	< 15%	12.7%
Wafer Handler Precision	+/- 200 μ m mean 3 sigma	53 μ m mean 3 sigma
Template change	< 30 minutes	~ 15 minutes
Wafer throughput	2 wph (200 mm)	1 wph (200 mm)

Table 2. Miscellaneous specifications

3.5 Upgrades to the Imprio-100

Since the delivery of the Imprio 100 to Motorola in July of 2003 several accessories and upgrade have been added. A dual dispense system for the etch barrier including necessary hardware and software have been installed. This provides the flexibility for using two different etch barriers depending on the desired processing application. The system was installed as a 200 mm wafer system and has been upgraded to allow processing on both 100 mm and 150 mm wafer sizes. Further upgrades are also being considered, such as a faster etch barrier dispense system and an automatic alignment scheme.

4. CONCLUSIONS

Acceptance testing of the first commercially available S-FIL tool has been completed. All specifications were met or exceeded for overlay, pre-align precision, residual layer thickness and uniformity, resolution, and lamp non-uniformity. Only the specification relating to wafer throughput was not met largely due to the long spread times needed to achieve minimal residual layer thickness. Several materials were explored for their performance as transfer layers. This evaluation demonstrated good spreading of the etch barrier and good interlayer adhesion for all of the transfer layers considered. Since installation and acceptance testing, several improvements and upgrades have been made to the Imprio 100 including a dual dispense system for the etch barrier, the capability to run wafer sizes of 100 mm and 150 mm wafers, and software upgrades.

ACKNOWLEDGEMENTS

The authors gratefully acknowledge William Dauksher and Kevin Nordquist for template fabrication. The authors wish to thank Ted Gehoski for his work in cleaning and reclaiming templates. The authors also extend their gratitude to Lester Casoose, and Mark Madrid, for providing overlay and SEM analysis. In addition, Philip Schumaker and Duc Nguyen are also acknowledged for their technical and service support. The authors would also like to extend their appreciation to Laura Siragusa and Vida Ilderem for their support in this work. This work was partially funded by DARPA (N66001-02-C-8011, N66001-01-1-8964).

REFERENCES

1. International Technology Roadmap for Semiconductors, 2003 Edition.
2. S. Y. Chou, P. R. Krauss, P. J. Renstrom, *J. Vac. Sci. Technol. B* 1996, 14(6), 4129-4133.
3. M. Bender et al., "Multiple Imprinting in UV based Nanoimprint Lithography: Related Materials Issues," *Microelectronic Engineering*, 61-62 (2002), pp. 407-413.
4. Colburn, M., Johnson, S., Stewart, M., Damle, S., Bailey, T., Choi, B.J., Wedlake, M., Michaelson, T., Sreenivasan, S.V., Ekerdt, J., and Willson, C.G., "Step and Flash Imprint Lithography: A New Approach to High-Resolution Patterning," *Proc. of SPIE*, vol. **3676**, pp. 379-389, March 1999.
5. D. J. Resnick, W. J. Dauksher, D. Mancini, K. J. Nordquist, E. Ainley, K. Gehoski, J. H. Baker, T. C. Bailey, B. J. Choi, S. Johnson, S. V. Sreenivasan, J. G. Ekerdt, and C. G. Willson, *Proc. SPIE* 4688, 205 (2002).
6. I. McMackin, P. Schumaker, D. Babbs, J. Choi, W. Collison, S. V. Sreenivasan, N. Schumaker, M. Watts, R. Voisin, *Proc. SPIE*, vol. 5037, pp. 178 – 186, (2003).
7. W. J. Dauksher, D. P. Mancini, K. J. Nordquist, D. J. Resnick, D. L. Standfast, D. Convey, and Y. Wei, *J. Vac. Sci. Technol. B* **21**, 2771 (2003)
